
Gaia DR 2 data and the evolutionary status of eight high velocity hot post-AGB candidates

Mudumba PARTHASARATHY^{1,2}, Tadafumi MATSUNO³ and Wako AOKI^{2,3}

¹Indian Institute of Astrophysics, II Block, Koramangala, Bangalore 560 034, INDIA

²National Astronomical Observatory, 2-21-1 Osawa, Mitaka, Tokyo 181-8588, Japan

³Department of Astronomical Science, School of Physical Sciences, The Graduate University of Advanced Studies (SOKENDAI), 2-21-1 Osawa, Mitaka, Tokyo 181-8588, Japan

*E-mail: m-partha@hotmail.com, matsuno@astro.rug.nl, aoki.wako@nao.ac.jp

Received (reception date); Accepted (acceptation date)

Abstract

From *Gaia* DR 2 data of eight high velocity hot post-AGB candidates LS 3593, LSE 148, LS 5107, HD 172324, HD 214539, LS IV -12 111, LS III +52 24, and LS 3099, we found that six of them have accurate parallaxes which made it possible to derive their distances, absolute visual magnitudes (M_V) and luminosity ($\log L/L_\odot$). Except LS 5107 all the remaining seven stars have accurate effective temperature (T_{eff}) in the literature. Some of these stars are metal-poor and some of them do not have circumstellar dust shells. In the past the distances of some stars were estimated to be 6 kpc which we find it to be incorrect. The accurate *Gaia* DR2 parallaxes show that they are relatively nearby post-AGB stars. When compared with post-AGB evolutionary tracks we find their initial masses in the range of $1 M_\odot$ to $2 M_\odot$. We find the luminosity of LSE 148 to be significantly lower than that of post-AGB stars, suggesting that this is a post-horizontal branch star or post-early-AGB star. LS 3593 and LS 5107 are new high velocity hot post-AGB stars from *Gaia* DR2.

Key words: stars:evolution — stars:AGB and post-AGB — stars:high-velocity — stars:distances

1 Introduction

Hot post-AGB stars are transition objects evolving towards the early stages of planetary nebulae (PNe) (Kwok 1993; van Winckel 2003; Parthasarathy 2006; Parthasarathy et al. 1993; Parthasarathy et al. 1995, and references therein). Some of the hot post-AGB stars are at high galactic latitudes and a few are high velocity stars, e.g., LS III +52 24 (IRAS 22023+5249: $V_r = -148 \text{ km s}^{-1}$; Sarkar et al. 2012), LS 5112 (IRAS 18379-1707: $V_r = -124 \text{ km s}^{-1}$; Ikonnikova et al. 2020). These stars could be highly evolved low-mass metal-poor stars in the halo population of the Milky Way. Determination of evolutionary status and frequency of these objects is useful for better understanding of both low-mass star evolution and the Milky Way halo structure.

Hence, these objects prompted us to look for more such stars. However the radial velocities and distances of most of the hot post-AGB candidates were not available. With the advent of *Gaia* DR 2 data (Gaia Collaboration et al. 2018; Lindegren et al. 2018) one can look for more such stars.

We considered the hot post-AGB candidates given in the following papers: Mello et al. (2012); Venn et al. (1998); Kendall et al. (1994); Przybylski (1969); Klochkova et al. (2018); Sarkar et al. (2005); Sarkar et al. (2012). From the *Gaia* DR 2 data we found LS 3593 (SAO 243754), LSE 148 (HD 177566), LS 5107 (IRAS 18365-1353), HD 172324 (V 534 Lyr), HD 214539, and LS 3099 to be high velocity stars with accurate *Gaia* DR 2 parallaxes (see Tables 1 and 2). LS IV -12 111 and LS III +52 24 do not have accurate parallaxes. We also looked at the proper motion data of these eight stars in the *Gaia* DR 2.

In this paper we analyze the *Gaia* DR 2 data of the above mentioned eight stars and based on it we discuss their evolutionary status.

2 Data and analysis

The Galactic longitude and latitude, parallaxes, radial velocities, G (*Gaia* G band), V , $B - V$ and spectral types of all the eight stars mentioned above are given in Table 1. The data are taken from SIMBAD and *Gaia* DR2.

Using the *Gaia* DR 2 parallaxes the distances are derived (Table 2). The $E(B - V)$ values (Table 2) are obtained from Schlegel et al. (1998) for high galactic latitude stars (LSE 148, HD172324, HD214539). The interstellar reddening of these three stars is quite small. Chen et al. (2019) and Green et al. (2018) are used for LS3593 and LS5107, respectively. Extinction coefficients are converted using values provided in Green et al. (2018), Schlafly, & Finkbeiner

(2011), and mean values in Casagrande, & Vandenberg (2018). Table 2 lists $E(B - V)$ obtained from dust map as well as $E(B - V)$ values calculated from the observed $(B - V)$ and intrinsic $(B - V)$ obtained from their spectral types ($E(B - V)_{\text{sp}}$). The $E(B - V)_{\text{sp}}$ values of three IRAS sources are 0.09 – 0.32 mag larger than the $(E - V)$ estimated from the dust map. This suggests that they are affected by circumstellar reddening, in addition to the interstellar reddening.

The calculated absolute visual magnitudes M_V are given in Table 2. For M_V values we applied bolometric corrections as the T_{eff} values and spectral types of all the stars are well determined. The bolometric corrections were taken from Allen’s Astrophysical Quantities (4th edition; Cox 2000). The values of the bolometric corrections of Flower (1996) are 0.1–0.25 magnitude larger than those of the Allen’s Astrophysical Quantities, resulting in difference in $\log L/L_{\odot}$ by less than 0.1 dex. This does not affect the discussion on the nature of our high velocity post-AGB stars. The derived bolometric magnitudes M_{bol} and $\log L/L_{\odot}$ values are given in Table 2. Notes on all the eight stars are given below.

Stellar parameters, i.e. T_{eff} , $\log g$, and $[\text{Fe}/\text{H}]$ are given in Table 2. Details of these parameters and references will be provided for individual objects below.

Kinematics are calculated using *Gaia* parallax and proper motion measurements. We adopt 8.2 kpc as the distance between the Sun and the Galactic center (McMillan 2017), 0.025 kpc as the vertical offset of the Sun (Jurić et al. 2008). Solar motion is adopted from Schönrich et al. (2010) for the radial and vertical velocities (11.1 km s^{−1} and 7.25 km s^{−1}, respectively) and is calculated as 247.97 km s^{−1} using the proper motion measurements by Reid, & Brunthaler (2004). The results are presented in Table 3.

From the radial velocity measurements by previous studies, no clear signature of binarity has been found for these stars. The constraint is still not very strong due to the limitation of the number of spectroscopic observations. We note that the sample selection of high velocity post-AGB stars would not be affected if they belong to low-mass star binaries because the radial velocity variations expected for low-mass star binaries are not as large as the radial velocity of the stars studied in this paper.

2.1 Notes on the eight stars

- LS 3593

Venn et al. (1998) derived $T_{\text{eff}} = 9300$ K, $\log g = 1.7$. They have derived chemical composition of this star. They found it to be metal-poor ($[\text{Fe}/\text{H}] = -2.0$). Oxygen and nitrogen seem to be slightly overabundant. They do not find any emission lines in the spectrum. They found

it to be a very slow rotator. Its galactic latitude is low but is found to be a high velocity star.

- LSE 148

It is a high galactic latitude and high velocity star (Table 1). Kendall et al. (1994) derived $T_{\text{eff}} = 30,600$ K and $\log g = 3.5$. They find it to be metal-poor. Carbon is underabundant similar to that observed in high galactic latitude hot post-AGB stars. They conclude that it is a hot post-AGB star of core mass $0.55M_{\odot}$. They find it to be a very slow rotator. No emission lines are present in the spectrum. Mello et al. (2012) also find it to be very metal-poor. They find weak emission in the cores of Balmer lines. Mello et al. (2012) derived $T_{\text{eff}} = 30,900$ K, $\log g = 3.8$ which agrees well with the results obtained by Kendall et al. (1994). Mello et al. (2012) find no Fe lines in the spectrum of LSE 148. They suggested that it may be a post-horizontal branch star or a post-early AGB star. This is supported by the present work with much robust estimate of the luminosity (see Sect. 3).

- LS 5107 (IRAS 18365-1353)

There is no detailed study of the spectrum of this star. Venn et al. (1998) find that $H\alpha$ line to be a P-Cygni profile and find Fe II emission line at 6515 \AA . LS 5107 is found to be an IRAS source with far-IR colors similar to that of post-AGB stars and planetary nebulae. The T_{eff} given in Table 2 is estimated from its spectral type. We conclude that LS 5107 is a high velocity hot post-AGB star.

- HD 172324 (V534 Lyr)

It is a high galactic latitude and high velocity star (Table 1). It is a small amplitude light and radial velocity variable. Recently, Klochkova et al. (2018) made detailed analysis of the high resolution spectra of this star and derived its chemical composition. They find $T_{\text{eff}} = 10,000$ K, $\log g = 2.5$. They find it to be metal-poor and overabundant in nitrogen. The $H\alpha$ line shows variable P-Cygni profile. They conclude that it is a population-II pulsating star near the horizontal branch. Klochkova et al. (2018) derived a distance of 6 kpc, whereas Bonsack, & Greenstein (1956) estimated a distance of 5.7 kpc. The *Gaia* DR 2 data (Tables 1 and 2), however, clearly shows that their distance estimate is wrong. The luminosity estimated from this distance is well higher than the value expected for the horizontal branch stars. We note that the $\log g$ value derived by spectroscopic analysis by Klochkova et al. (2018) is also lower than the typical values of horizontal branch stars.

- HD 214539

It is a high galactic latitude and very high velocity star (Table 1). Przybylski (1969) made a detailed analysis of the spectrum of this star. He finds it to be a metal-poor ($[\text{Fe}/\text{H}] = -1.2$)

and low gravity star. It is considered at that time the brightest known blue halo star. Kodaira, & Philip (1984) derived $T_{\text{eff}} = 9800$ K and $\log g = 1.6$.

- LS 3099 (IRAS 13266-5551)

Mello et al. (2012) and Sarkar et al. (2005) analyzed the high resolution spectrum of this B1 Iae post-AGB star. They find $T_{\text{eff}} = 20,200$ K, $\log g = 2.38$ and mildly carbon-poor and metal-poor Mello et al. (2012). The radial velocity is found to be 65.31 ± 0.34 km s⁻¹ (Sarkar et al. 2005).

- LS IV -12 111 (IRAS 19590-1249)

It is a high galactic latitude ($b = -21.26$ degrees) and high velocity (86.9 km s⁻¹) hot (B1Iae) post-AGB star. Ryans et al. (2003) and Mello et al. (2012) analyzed high resolution spectrum of this star. They derive $T_{\text{eff}} = 20,500$ K and $\log g = 2.5$ (Ryans et al. 2003). The values derived by Mello et al. (2012) are in agreement with the results of Ryans et al. (2003). They find it to be carbon-poor by ~ 0.4 dex similar to that found in high galactic latitude OB post-AGB stars, indicating that the star left the AGB before the third dredge-up. The parallax of this object in *Gaia* DR2 is not sufficiently accurate.

- LS III +52 24 (IRAS 22023+5249)

Sarkar et al. (2012) analyzed high resolution spectrum of this hot (B1 I) post-AGB star. They find the radial velocity to be -148.31 ± 0.60 km s⁻¹. They derive $T_{\text{eff}} = 24,000 \pm 1000$ K, $\log g = 3.0 \pm 0.5$ and -0.12 dex metal-poor. The spectrum shows nebular emission lines indicating the presence of a low excitation planetary nebula. Arkhipova et al. (2013) find small amplitude light variations similar to that found in other post-AGB stars. The parallax of this object in *Gaia* DR2 is not sufficiently accurate.

3 Discussion

We show in Figure 1 the location of six high velocity stars in the HR diagram. LS IV -12 111 and LS III +52 24 parallaxes are not determined with accuracy of three sigma, hence, they are not shown in Figure 1. Four of the six stars have similar T_{eff} and L along the evolutionary tracks of low-mass post-AGB stars.

Kinematics show that all stars except LS 5107 do not follow the Galactic rotation. LS 5107, for which there is no estimate of metallicity, could belong to the thin disk, according to the kinematics information. LSE 148 and HD 214539 show large velocities relative to the Sun, and hence they would belong to the Galactic halo, indicating that their initial masses are low. The other three, LS 3593, HD172324 and LS 3099 show modest relative velocities compared

to the Sun. Although they could belong to the Galactic disk, it is unlikely that their ages are young given the age-velocity dispersion relation among Milky Way disk stars (e.g., Casagrande et al. 2011). These kinematics features are consistent with the results from the positions in the $T_{\text{eff}}\text{-log } L$ plane that these stars are low-mass halo post-AGB objects.

LSE 148 has luminosity that is even lower than that of low-mass post-AGB stars. This suggests that this is a post-horizontal branch star or post-early-AGB star.

LS 3099 has luminosity explained by post-AGB stars with about $2.0M_{\odot}$ and is not metal-poor. This star may be a thick disk star with relatively high metallicity.

Although LS IV-12 111 and LS III +52 24 do not have reliable parallax measurements, we can place lower limits on their tangential velocities. The 2σ lower limits are $108 \text{ (kms}^{-1}\text{)}$ and $118 \text{ (kms}^{-1}\text{)}$. These results, together with their large radial velocities, support that these stars are high-velocity stars.

3.1 Frequency of metal-poor post-AGB stars and timescale of evolution

We find four metal-poor post-AGB stars with low core masses ($\sim 0.55M_{\odot}$, which corresponds to initial masses of $1.0M_{\odot}$ or smaller). They have $T_{\text{eff}} \sim 10000 \text{ K}$. Taking account of the incompleteness of the sample of this study, this can be used to estimate the lower limit of the frequency of such objects in the Galaxy. The distances of these objects are about 2 kpc or less, which became available by the *Gaia* DR2 for the first time. The local stellar density of the halo structure is estimated to be $3 - 15 \times 10^{-5} M_{\odot} \text{ pc}^{-3}$ (Deason et al. 2019 and references therein). Adopting the recent estimate, $7 \times 10^{-5} M_{\odot} \text{ pc}^{-3}$, by Deason et al. (2019), the stellar halo mass within 2 kpc is $1.7 \times 10^6 M_{\odot}$. Hence, the frequency of metal-poor post-AGB stars is the order of 10^{-6} . If higher luminosity (larger distance) was applied as estimated by previous studies for some of our post-AGB stars, the frequency could be much lower. Taking account of the lifetime of such low-mass stars is $\sim 10^{10}$ years, the time-scale of the evolution in this phase is estimated to be 10^4 years. This roughly agrees with the prediction of the recent model calculation of Miller Bertolami (2016) shown in their Figure 8 for metal-poor low-mass stars.

Since the timescale of the evolution of low-mass metal-poor objects is even longer from 10000 K to the maximum effective temperature ($\sim 100,000 \text{ K}$), hotter high velocity post-AGB stars with low-metallicity could exist in the Milky Way halo that are yet identified. Further searches for such stars will provide useful constraint on the frequency of low-mass metal-poor post-AGB stars.

Acknowledgments

MP was supported by the NAOJ Visiting Fellow Program of the Research Coordination Committee, National Astronomical Observatory of Japan (NAOJ), National Institutes of Natural Sciences(NINS).

References

- Arhipova, V. P., Burlak, M. A., Esipov, V. F., et al. 2013, *Astronomy Letters*, 39, 619
- Bonsack, W. K., & Greenstein, J. L. 1956, *PASP*, 68, 249
- Casagrande, L., Schönrich, R., Asplund, M., et al. 2011, *A&A*, 530, A138
- Casagrande, L., & VandenBerg, D. A. 2018, *MNRAS*, 479, L102
- Chen, B.-Q., Huang, Y., Yuan, H.-B., et al. 2019, *MNRAS*, 483, 4277
- Cox, A. N. 2000, *Allen's Astrophysical Quantities*
- Deason, A. J., Belokurov, V., & Sanders, J. L. 2019, *MNRAS*, 490, 3426
- Dorman, B., Rood, R. T., & O'Connell, R. W. 1993, *ApJ*, 419, 596
- Flower, P. J. 1996, *ApJ*, 469, 355
- Gaia Collaboration, Brown, A. G. A., Vallenari, A., et al. 2018, *A&A*, 616, A1
- Green, G. M., Schlafly, E. F., Finkbeiner, D., et al. 2018, *MNRAS*, 478, 651
- Ikonnikova, N. P., Parthasarathy, M., Dodin, A. V., et al. 2020, *MNRAS*, 491, 4829
- Jurić, M., Ivezić, Ž., Brooks, A., et al. 2008, *ApJ*, 673, 864
- Kendall, T. R., Brown, P. J. F., Conlon, E. S., et al. 1994, *A&A*, 291, 851
- Klochkova, V. G., Sendzikas, E. G., & Chentsov, E. L. 2018, *Astrophysical Bulletin*, 73, 52
- Kodaira, K., & Philip, A. G. D. 1984, *ApJ*, 278, 208
- Kwok, S. 1993, *ARA&A*, 31, 63
- Lindgren, L., Hernández, J., Bombrun, A., et al. 2018, *A&A*, 616, A2
- McMillan, P. J. 2017, *MNRAS*, 465, 76
- Mello, D. R. C., Daflon, S., Pereira, C. B., et al. 2012, *A&A*, 543, A11
- Miller Bertolami, M. M. 2016, *A&A*, 588, A25
- Parthasarathy, M. 2006, *Planetary Nebulae in our Galaxy and Beyond*, 234, 79
- Parthasarathy, M., Garcia-Lario, P., de Martino, D., et al. 1995, *A&A*, 300, L25
- Parthasarathy, M., Garcia-Lario, P., Pottasch, S. R., et al. 1993, *A&A*, 267, L19
- Przybylski, A. 1969, *MNRAS*, 146, 71
- Reid, M. J., & Brunthaler, A. 2004, *ApJ*, 616, 872
- Ryans, R. S. I., Dufton, P. L., Mooney, C. J., et al. 2003, *A&A*, 401, 1119
- Sarkar, G., García-Hernández, D. A., Parthasarathy, M., et al. 2012, *MNRAS*, 421, 679

- Sarkar, G., Parthasarathy, M., & Reddy, B. E. 2005, *A&A*, 431, 1007
- Schlafly, E. F., & Finkbeiner, D. P. 2011, *ApJ*, 737, 103
- Schlegel, D. J., Finkbeiner, D. P., & Davis, M. 1998, *ApJ*, 500, 525
- Schönrich, R., Binney, J., & Dehnen, W. 2010, *MNRAS*, 403, 1829
- van Winckel, H. 2003, *ARA&A*, 41, 391
- Venn, K. A., Smartt, S. J., Lennon, D. J., et al. 1998, *A&A*, 334, 987

Table 1. Objects

| Object | l (degree) | b (degree) | Parallax(p) (mas) | V_r (km s ⁻¹) | G (mag) | V (mag) | $B - V$ (mag) | spectral type | Note |
|---------------|-----------------|-----------------|--------------------------|--------------------------------|--------------|--------------|------------------|---------------|-------------------------|
| LS 3593 | 330.6439866 | -3.672106351 | 0.410±0.047 | 110.12±1.94 | 9.44 | 9.53 | 0.15 | B8Iab | |
| LSE 148 | 355.54719 | -20.42079462 | 0.697±0.106 | -134.00±4.30 | 10.15 | 10.17 | -0.20 | B6Ib | |
| LS 5107 | 19.24285127 | -3.663147838 | 0.624±0.052 | -76.65±8.30 | 9.52 | 9.89 | 0.86 | B9Iae | V452 Sct IRAS source |
| HD 172324 | 66.18384285 | 18.58124629 | 0.456±0.042 | -117.10±2.00 | 8.14 | 8.16 | 0.01 | A0Iabe | V534 Lyr |
| HD 214539 | 319.7541249 | -44.93459676 | 0.719±0.041 | 333.00±2.80 | 7.18 | 7.25 | 0.00 | B9Ib/A0Iab | |
| LS 3099 | 308.3016934 | 6.35580537 | 0.377±0.050 | 65.31±0.34 | 10.70 | 10.68 | 0.39 | B1Iae | IRAS source |
| LS IV-12 111 | 29.17960346 | -21.2637799 | 0.129±0.055: | 86.9±1.7 | 11.32 | 11.4 | -0.1 | B1Iae | IRAS source |
| LS III +52 24 | 99.30346632 | -1.955656239 | 0.080±0.052: | -148.31±0.60 | 12.36 | 12.51 | 0.72 | B1I | IRAS source |

Table 2. Distance and stellar parameters

| Object | Distance(D) (pc) | $E(B - V)$ (mag) | $E(B - V)_{sp}$ (mag) | M_V (mag) | M_g (mag) | $\log L/L_\odot$ | T_{eff} (K) | $\log g$ | [Fe/H] | references |
|--------------|-------------------------|---------------------|--------------------------|----------------|----------------|------------------|------------------|----------|--------|------------|
| LS 3593 | 2436±281 | 0.21 | 0.18 | -2.97 | -3.07±0.26 | 3.35±0.11 | 9300 | 1.7 | -2.0 | 1 |
| LSE 148 | 1436±219 | 0.10 | 0.07 | -0.08 | -0.91±0.34 | 2.59±0.14 | 30900 | 3.8 | < -2.0 | 2 |
| LS 5107 | 1602±135 | 0.56 | 0.88 | -2.64 | -3.04±0.19 | 3.17±0.09 | 10500 | 2.0 | ... | |
| HD 172324 | 2194±202 | 0.06 | 0.02 | -3.71 | -3.73±0.21 | 3.54±0.09 | 10000 | 2.5 | -0.3 | 3 |
| HD 214539 | 1392±80 | 0.03 | 0.02 | -3.55 | -3.62±0.14 | 3.53±0.07 | 9800 | 1.6 | < -1.5 | 4,5 |
| LS 3099 | 2650±351 | 0.33 | 0.51 | -3.12 | ... | 3.67±0.12 | 20200 | 2.38 | | |
| LS IV-12 111 | > 4180 | 0.19 | 0.28 | < -2.32 | < -2.32 | > 3.63 | 20500 | 2.5 | | |
| LS III 52-24 | > 5398 | 0.67 | 0.64 | < -2.95 | < -3.14 | > 3.92 | 24000 | 3.0 | | |

References – 1:Venn et al. (1998); 2: Mello et al. 2012; 3: Klochkova et al. (2018); 4: Kodaira, & Philip (1984); 5:Przybylski (1969)

Table 3. Kinematics data

| Object | μ_α (mas) | $\sigma(\mu_\alpha)$ (mas) | μ_δ (mas) | $\sigma(\mu_\delta)$ (mas) | V_R (km s ⁻¹) | $\sigma(V_R)$ (km s ⁻¹) | V_ϕ (km s ⁻¹) | $\sigma(V_\phi)$ (km s ⁻¹) | V_Z (km s ⁻¹) | $\sigma(V_Z)$ (km s ⁻¹) |
|--------------|-----------------------|-------------------------------|-----------------------|-------------------------------|--------------------------------|--|-----------------------------------|---|--------------------------------|--|
| LS 3593 | -4.252 | 0.066 | -11.621 | 0.053 | -56.85 | 7.44 | 78.13 | 11.73 | -56.17 | 6.27 |
| LSE 148 | -2.030 | 0.167 | -42.817 | 0.157 | 163.10 | 7.89 | -8.18 | 34.46 | -17.97 | 10.04 |
| LS 5107 | -4.487 | 0.082 | -6.045 | 0.074 | -83.46 | 7.52 | 228.88 | 4.71 | 11.15 | 0.83 |
| HD 172324 | -3.183 | 0.079 | -0.969 | 0.080 | 68.09 | 3.74 | 144.65 | 2.31 | -61.38 | 3.23 |
| HD 214539 | -25.891 | 0.057 | -26.177 | 0.065 | -320.38 | 7.23 | -31.02 | 8.53 | -63.93 | 9.96 |
| LS 3099 | -5.69 | 0.074 | -2.744 | 0.079 | -39.7 | 2.0 | 146.7 | 5.1 | -6.9 | 3.2 |
| LS IV-12 111 | -3.596 | 0.094 | -4.096 | 0.061 | | | | | | |
| LS III 52-24 | -3.856 | 0.100 | -2.566 | 0.070 | | | | | | |

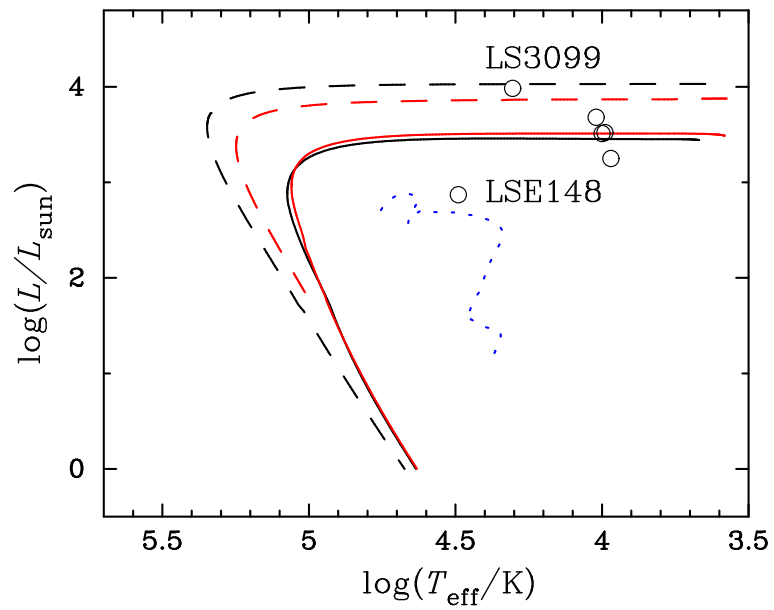


Fig. 1. Evolutionary tracks of post-AGB phases taken from Miller Bertolami (2016) for initial masses of $1.0 M_{\odot}$ (solid lines) and $2.0 M_{\odot}$ (dotted lines) with $Z = 0.02$ (red) and $Z = 0.001$ (black). The evolutionary track of post-horizontal branch star for the core mass of $0.52 M_{\odot}$ with $[\text{Fe}/\text{H}] = -1.48$ taken from Dorman et al. (1993) is shown by dotted (blue) line. The six object studied in the present work are shown by open circles.